Homotopy Method for Optimal Motion Planning With Homotopy Class Constraints

Wenbo He, Yunshen Huang, Jie Wang, and Shen Zeng

***Abstract*—Optimal motion planning is an essential task within the field of control theory. Therein, the key task is to synthesize optimal system trajectories that pass through cluttered environments while respecting given homotopy class constraints, which is critical in many topology-restricted applications such as search and rescue. In this letter, we introduce a novel optimal motion planning technique with 2-dimensional homotopy class constraints for general dynamical systems. We first initialize an optimal system trajectory regardless of obstacles and homotopy class constraints, and design an auxiliary obstacle trajectory for each obstacle such that the system trajectory belongs to the desired homotopy class regarding these auxiliary obstacle trajectories. During the procedure of deforming the auxiliary obstacle trajectory to the original counterparts, we propose a homotopy method based on nonlinear programming (NLP) such that the synthesized optimal system trajectories fulfill the aforementioned homotopy class constraints. The proposed method is validated with numerical results on two classic nonlinear systems with planar static and moving obstacles.**

***Index Terms*—Optimal motion planning, homotopy class constraints, nonholonomic systems.**

I. Introduction

MOTION planning aims to provide a motion strategy that drives a dynamic system from a given starting state to a desired target state without colliding with obstacles. It has attracted significant research interest in the past few decades and is still actively studied in the robotics field. In this letter, we additionally consider the minimum energy consumption during the movements for optimal control.

For simple holonomic systems whose feasible moving dimension is equal to the work space's dimension, many sampling-based motion planning algorithms can be deployed even in a nonconvex environment, such as probabilistic roadmaps (PRM) [1] and rapidly-exploring random trees (RRT) [2]. When systems are nonholonomic, methods such as iterative method [3] and sequential homotopy quadratic programming (SHQP) [4] can be leveraged to address the motion planning problems. However, these algorithms lack the consideration of possible topological constraints that are commonly seen. For instance, in a drone surveillance task, a quadcopter is commanded to patrol a building by encircling it twice before reaching the landing spot. Such two encirclements in a specified direction, which are critical for this surveillance task, is formally defined as a homotopy class constraint. Moreover, homotopy class constraints can be leveraged to find the global optimal trajectory in a cluttered environment [5].

Several pioneering works have shown promising results in dealing with motion planning problems with homotopy class constraints. Geometric methods [6] are capable of classifying homotopy classes in two-dimensional environments. Furthermore, the search-based method [7] improves the classification in higher-dimensional space and synthesizes feasible trajectories fulfilling the homotopy class constraints. In addition, a PRM-based method [8] and Mixed integer programming (MIP) algorithms [5], [9] are proposed. The authors of [7] leverage h-signature to generate optimal trajectories that fulfill the homotopy class constraints. However, the application of these pioneering algorithms is limited to linear systems or extremely simplified nonlinear systems, which may hinder their practicality. In [10], we proposed the auxiliary energy reduction technique for addressing motion planning problems with homotopy class constraints, which is applicable to general nonlinear systems. However, it only focuses on the feasibility of the trajectory, whereas no optimality is considered.

In this letter, we propose a novel direction that addresses the optimal motion planning task with 2-dimensional homotopy class constraints for general nonlinear nonholonomic dynamical systems with both static and moving obstacles. We first initialize an optimal trajectory of the dynamical system without considering obstacles, then we design the auxiliary trajectories of obstacles such that the initial system trajectory is collision-free and belongs to the desired homotopy class regarding the auxiliary obstacle trajectories. Next, we iteratively deform auxiliary obstacle trajectories to the original ones and determine the optimal system trajectory accordingly. Having done so, the resulting trajectory is feasible and satisfies homotopy class constraints regarding the original obstacles.

This letter is organized as follows. Section II introduces the problem setup and mathematical preliminaries. We then provide the method of auxiliary obstacle trajectory synthesizing in Section III. The overall algorithm is given in Section IV. We present the numerical results in Section V and conclude this letter in Section VI.

Manuscript received 16 September 2022; revised 12 November 2022; accepted 29 November 2022. Date of publication 14 December 2022; date of current version 29 December 2022. This work was supported by NSF under Grant CMMI-1933976. Recommended by Senior Editor M. Arcak. *(Corresponding author: Shen Zeng.)*

The authors are with the Department of Electrical and System Engineering, Washington University, St. Louis, MO 63130 USA (e-mail: wenbo.he@wustl.edu; yunshen.huang@wustl.edu; jie.w@wustl.edu; s.zeng@wustl.edu).

Digital Object Identifier 10.1109/LCSYS.2022.3228898

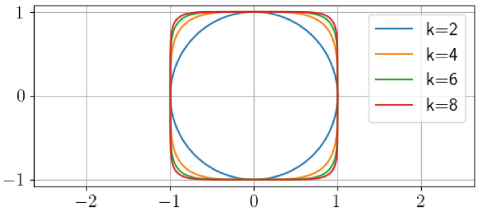

Fig. 1. One obstacle approximation with $(z_x, z_y) = (0, 0)$, $r_x = r_y = R = 1$. As k increases, the obstacle turns more toward a rounded square.

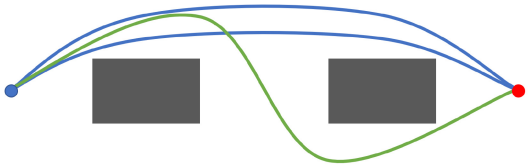

Fig. 2. The three curves are the trajectories connecting identical starting and target points, and grey rectangles are obstacles. According to the definition of the homotopy class, the two blue trajectories are homotopy equivalent, but the green one belongs to a different homotopy class.

II. Mathematical Preliminaries and Problem Statement

A. Differentiable Obstacle Representations

Consider M number of moving obstacles which can be of any shape or size, in a 2-dimensional cluttered environment. An often-faced challenge is non-differentiable shapes such as a square and triangle that can not be directly handled by nonlinear programming. To address this issue, we approximate non-differentiable obstacles using super-ellipses [4], which in turn yields the collision avoidance constraints

$$\left(\frac{x(t) - z_{ix}(t)}{r_{ix}}\right)^{k_i} + \left(\frac{y(t) - z_{iy}(t)}{r_{iy}}\right)^{k_i} - {R_i}^{k_i} \geq 0, \tag{1}$$

where $z(t) = [z_{ix}(t), z_{iy}(t)]$ denotes the center of the i^{th} obstacle at time t. $r_{ix}, r_{iy} \geq 1$ represent the object's spatial extensions, and $[x(t), y(t)]$ is the trajectory of the dynamical system. $R_i > 0$ is a size constant and the exponent k_i is a positive even number. If $k_i = 2$, the obstacle is a circle or an ellipse, otherwise a rounded square, as shown in Figure 1.

B. Optimal Motion Planning

The basic task of motion planning is to find a dynamically feasible trajectory that connects the given starting and target points while satisfying some obstacle constraints imposed by the environment. The task of optimal motion planning further requires the synthesized trajectory to be optimal, or locally optimal, with respect to a certain metric such as energy consumption. Generally, the optimal trajectory can be obtained by solving the following nonlinear program:

$$\begin{aligned} \underset{(x(\cdot),u(\cdot))}{\text{minimize}} \quad & \Phi(x(\cdot), u(\cdot)) \\ \text{subject to} \quad & x(0) = x_{\text{start}}, \ x(T) = x_{\text{target}} \\ & \dot{x}(t) = f(x(t), u(t)) \\ & G(x(t)) \geq 0, \quad \forall t \in [0, T], \end{aligned} \tag{2}$$

where $x(t) \in \mathbb{R}^n, u(t) \in \mathbb{R}^m$ are the state and control input respectively. Φ is the loss function, $f : \mathbb{R}^n \times \mathbb{R}^m \to \mathbb{R}^n$ describes the system dynamics, and $G(x(t)) \geq 0$ is the control barrier function which defines a collision-free space. In this letter, we focus on energy-optimal motion planning such that $\Phi(x(\cdot), u(\cdot)) = \int_0^T \|u(t)\|^2 dt$ while the total time T is pregiven, but it is straightforward to modify the nonlinear program to further accommodate the time-optimal requirement.

C. Homotopy Class Constraints for Movable Obstacles

Collision avoidance of movable obstacles is critical in some topology-restricted tasks, e.g., a vehicle properly avoids other cars while merging off a highway. In this example, an appropriate route fulfilling the homotopy class constraints for movable obstacles, i.e., other in-moving cars, is desired.

Definition 1: Two trajectories belong to the same homotopy class if and only if they have identical start and target points and they can be smoothly deformed into one another without intersecting any obstacles.

Definition 1 is schematically shown in Figure 2.

Given a nominal 2-dimensional trajectory, one homotopy class is specified and such a constraint should be preserved throughout the iterative optimization process. However, obstacles being movable imposes more challenges to the homotopy class constraint guarantee as both obstacles and the trajectory of the given dynamical system are changing over time. We hence first define the homotopy class constraints under movable obstacle scenarios here and further prove that the proposed approach can preserve the desired homotopy class in Section III.

By virtue of the Residue Theorem [11], if the analytic function $F : \mathbb{C} \to \mathbb{C}$ does not have poles, and $c(t)$ is a continuous and closed curve on the complex plane that never intersects a point $z_0 \in \mathbb{C}$, then the following line integral holds,

$$\oint_c \frac{F(z)}{z - z_0} dz = 2\pi j F(z_0) n(c, z_0), \tag{3}$$

where j is the imaginary unit, $n(c, z_0)$ is the winding number representing the total number of times that the curve c encircles counterclockwise around z_0. Therefore we have the followings.

Lemma 1: Two continuous trajectories c_1 and c_2 in the complex plane with identical start and target points belong to the same homotopy class regarding the obstacle at z_0, if and only if

$$\oint_{c_1 \sqcap c_2^-} \frac{F(z)}{z - z_0} dz = 0,$$

where $c_1 \sqcap c_2^-$ is a closed trajectory concatenating c_1 and inverse c_2, which starts from the start point of c_1 to the end point of c_1 along the trajectory c_1 and then travel from it to the start point along the trajectory c_2.

The proof can be seen in [7, Lemma 1]. Note that for any trajectory $c(t)$, we have $\oint_c \frac{F(z)}{z - z_0} dz = \oint_{c'} \frac{F(z + z_0)}{z} dz$, where $c'(t) = c(t) - z_0$. In addition, we are able to heuristically generalize the criterion to a moving obstacle. More specifically, trajectories $c_1(t)$ and $c_2(t)$ belong to the same homotopy class regarding a obstacle trajectory $z_0(t)$, if and only if

$$\oint_{c_1' \sqcap c_2'^-} \frac{1}{z} dz = 0,$$

where $c'_1(t) = c_1(t) - z_0(t)$, $c'_2(t) = c_2(t) - z_0(t)$ and $F(z)$ is simply chosen as a constant map to 1. Note that if the obstacle trajectory is time-invariant, i.e., $z_0(t) \equiv z_0(0)$, this criterion also degenerates to the form of Lemma 1. Moreover, in a cluttered environment with multiple obstacles, this criterion becomes

$$\begin{bmatrix} \oint_{c'_{1,1} \sqcap c'^{-}_{2,1}} \frac{1}{z} dz \\ \vdots \\ \oint_{c'_{1,M} \sqcap c'^{-}_{2,M}} \frac{1}{z} dz \end{bmatrix} = \mathbf{0}_{M \times 1}, \tag{4}$$

where $c'_{1,i}(t) = c_1(t) - z_i(t)$ and $c'_{2,i}(t) = c_2(t) - z_i(t)$, and $z_i(t)$ is the trajectory of the i-th obstacle.

III. Auxiliary Obstacle Trajectory Synthesis

In this section, we propose a method of auxiliary obstacle trajectory synthesizing that guarantees the satisfaction of homotopy class constraints of the initial system trajectory towards these modified obstacles. In addition, we provide the condition under which this homotopy property holds while trajectories are deforming. All trajectories in this section are discussed on the complex plane for concise proof, but the results can be directly adopted in the $\mathbb{R}^2$ space. Let $z_i(t) = z_{ix}(t) + j \cdot z_{iy}(t)$ be the known trajectory of the center of the i-th movable obstacle and $r(t)$ be another given trajectory to specify the desired homotopy class. $r(t)$ is designed to never intersect the obstacles, i.e., $\|r(t) - z_i(t)\| > 0$ holds for all $i = 1, 2, \ldots, M$ and $t \in [0, T]$. A system trajectory $p(t)$ is acquired without concerning homotopy class constraints and obstacles but has the same start and target points as the ones of $r(t)$. Based on the notations, we define the auxiliary obstacle trajectory parameterized by s as

$$\hat{z}_i(t; s) = z_i(t) + s \frac{z_i(t) - r(t)}{\|z_i(t) - r(t)\|}, \tag{5}$$

where $s \in [0, \infty)$ is called the push distance. As $\|r(t) - z_i(t)\|_2 \geq R_i > 0$, $\forall t \in [0, T]$ because $r(t)$ is collision-free, we can choose a large-enough s_0 so that the conditions hold

$$\begin{aligned} \min_t \|\hat{z}_i(t; s_0)\| &> \max_t \|r(t)\| \\ \min_t \|\hat{z}_i(t; s_0)\| &> \max_t \|p(t)\|. \end{aligned} \tag{6}$$

A graphical example is demonstrated in Figure 3. We now show, according to (6), the sufficient condition that $p(t)$ and $r(t)$ belong to the same homotopy class with respect to $\hat{z}_i$.

Lemma 2: Given two continuous and closed trajectories $c_0(t)$ and $c_1(t)$ in the complex plane which never intersect the origin for $t \in [0, T]$, if there exists a continuous function $H(v, t)$ such that $H(0, t) = c_0(t)$, $H(1, t) = c_1(t)$, $\|H(v, t)\| \neq 0, \forall v \in [0, 1], \forall t \in [0, T]$, and $H(v, t)$ is the continuous and closed trajectory with any fixed $v \in [0, 1]$, then $\oint_{c_0} \frac{1}{z} dz = \oint_{c_1} \frac{1}{z} dz$.

Proof: Because $H(v, t)$ is continuous and never intersects the origin, $\theta(v) := \oint_{H(v,\cdot)} \frac{1}{z} dz$, $v \in [0, 1]$ is also continuous. According to the Residue Theorem [11], $\theta(v) = 2\pi j \cdot n(H(v, \cdot), 0)$ where $n(H(v, \cdot), 0) \in \mathbb{Z}$ is the winding number. Therefore the function $\theta(v)$ has to be both continuous and discrete, which implies $\theta(v)$ is constant, so that $\theta(0) = \theta(1)$. ■

Corollary 1: Given three trajectories $c_0(t)$, $c_1(t)$ and $\hat{z}(t)$ on the complex plane, where $c_0(0) = c_1(0)$, $c_0(T) = c_1(T)$, if $\min_t \|\hat{z}(t)\| > \max_t \|c_0(t)\|$ and $\min_t \|\hat{z}(t)\| > \max_t \|c_1(t)\|$, then $\oint_c \frac{1}{z} dz = 0$, where $c = (c_0 - \hat{z}) \sqcap (c_1 - \hat{z})^-$.

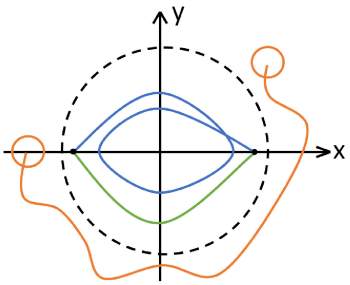

Fig. 3. Orange curve represents the auxiliary obstacle trajectory $\hat{z}(t)$. Trajectories $c_0(t)$ and $c_1(t)$ in blue and green, respectively, have the same start and target point. As the conditions $\min_t \|\hat{z}(t)\| > \max_t \|c_0(t)\|$ and $\min_t \|\hat{z}(t)\| > \max_t \|c_1(t)\|$ hold, they belong to the same homotopy class regarding the orange obstacle.

Proof: We define the continuous function

$$H_1(v, t) = \begin{cases} v \cdot c_0(t) - \hat{z}(t), & 0 \leq t \leq T \\ v \cdot c_1(2T - t) - \hat{z}(2T - t), & T < t \leq 2T \end{cases}$$

where $v \in [0, 1]$, $t \in [0, 2T]$. Therefore, $H_1(v, t)$ is the closed trajectory with any fixed $v \in [0, 1]$. For $v = 0$, $H_1(0, t)$ is a trivial trajectory that moves forth and back along $-\hat{z}$ such that $\oint_{H_1(0,\cdot)} \frac{1}{z} dz = 0$. $\|H_1(v, t)\| \geq \|\hat{z}(t)\| - s\|c_0(t)\| \geq \|\hat{z}(t)\| - \|c_0(t)\| > 0$ for $t \in [0, T]$, and similarly $\|H_1(v, t)\| > 0$ for $t \in [T, 2T]$. Therefore $H_1(v, t)$ never intersects the original point. Hence according to Lemma 2, $\oint_{H(1,\cdot)} \frac{1}{z} dz = \oint_{H(0,\cdot)} \frac{1}{z} dz = 0$, where $H(1, \cdot)$ is actually the closed curve concatenating $c_0 - \hat{z}$ and inverse $c_1 - \hat{z}$. ■

By virtue of Lemma 1 and Corollary 1, with a large s_0 that pushes the obstacle far enough so as to satisfy the conditions in (6), $p(t)$ and $r(t)$ are within the same homotopy class concerning the auxiliary obstacle trajectory $\hat{z}_i(t; s_0)$. The same idea can be directly generalized to the environment with multiple obstacles $\{z_1(t), \ldots, z_M(t)\}$, where a suitable s_0 is chosen for all obstacles. More specifically, the initialized system trajectory $p(t)$ and the pre-defined $r(t)$ belong to the same homotopy class with respect to a set of auxiliary obstacles trajectories $\{\hat{z}_1(t; s_0), \ldots, \hat{z}_M(t; s_0)\}$ as long as the conditions in (6) holds for every obstacle.

In the following, we aim to show how to obtain the trajectory that belongs to the same homotopy class of the given trajectory $r(t)$ towards original obstacle trajectories by deforming $p(t)$ and $\hat{z}_i(t; s)$ continuously.

Corollary 2: Given three trajectories $c_0(t; 0)$, $c_1(t; 0)$ and $\hat{z}(t; 0)$ on the complex plane that continuously deform to $c_0(t; 1)$, $c_1(t; 1)$ and $\hat{z}(t; 1)$ for $t \in [0, T]$, respectively. If $c_0(t; 0)$ and $c_1(t; 0)$ are homotopy equivalent towards $\hat{z}(t; 0)$, $c_0(0; v) = c_1(0; v), c_0(T; v) = c_1(T; v), \forall v \in [0, 1]$, and $c_0(t; v) \neq \hat{z}(t; v), c_1(t; v) \neq \hat{z}(t; v), \forall v \in [0, 1], \forall t \in [0, T]$ then $c_0(t; 1)$ and $c_1(t; 1)$ are homotopy equivalent towards $\hat{z}(t; 1)$.

Proof: We define the continuous function

$$H_2(v, t) = \begin{cases} c_0(t; v) - \hat{z}(t; v), & 0 \leq t \leq T \\ c_1(2T - t; v) - \hat{z}(2T - t; v), & T < t \leq 2T \end{cases}$$

where $v \in [0, 1]$, $t \in [0, 2T]$, then $H_2(v, t)$ is the closed trajectory with any fixed $v \in [0, 1]$. $H_2(v, t)$ never reaches the origin

because $c_0(t;v) \neq \hat{z}(t;v)$ and $c_1(t;v) \neq \hat{z}(t;v)$ always hold. Therefore according to the Lemma 2, $c_0(t;1)$ and $c_1(t;1)$ are homotopy equivalent towards $\hat{z}(t;1)$. ■

According to Corollary 2, during the continuous deformation of the auxiliary obstacle trajectories $\hat{z}_i(t;s)$ and the system trajectory $p(t)$, $p(t)$ remains within the same homotopy class of $r(t)$ if $\hat{z}_i(t;s)$ never intersects $p(t)$ and $r(t)$. Based on the definition (5), the deformation of $\hat{z}_i(t;s)$ can be controlled by $s \in [0,\infty)$. Therefore, by gradually decreasing s from s_0 to zero, i.e., $\hat{z}_i(t;s_0)$ is deformed to $\hat{z}_i(t;0) = z_i(t)$, and deforming $p(t)$ accordingly with no intersection, the resulting $p(t)$ also satisfies the homotopy class constraints regarding the original obstacles $z_i(t)$. It is noted that $\hat{z}_i(t;s)$ never intersects the predefined trajectory $r(t)$ in this deformation, which can be seen below:

$$\|\hat{z}_i(t;s) - r(t)\| = \left(1 + \frac{s}{\|z_i(t) - r(t)\|}\right)\|z_i(t) - r(t)\| > 0.$$

IV. Implemention With Optimal Control Criterion

In this section, we propose an algorithm to solve the problem of preserving the homotopy property from the last section by reformulating it into a sequence of nonlinear programming problems (NLP). The resulting NLP can be efficiently addressed by mature and off-the-shelf solvers and toolboxes such as CasADi [12]. In the following, we first describe a process of achieving optimal motion planning tasks with known obstacles using NLP. We next show how to prevent the system trajectories from intersecting the obstacles by transferring this task into sequential optimal motion planning problems.

A. Nonlinear Programming

To use the multiple shooting method, a continuous-time nonlinear dynamical system is discretized to the form

$$\begin{aligned} x(k+1) &= F(x(k), u(k)), \\ p(k) &= g(x(k)), \end{aligned} \tag{7}$$

where $x(k) := x(k\Delta T)$, $u(k) := u(k\Delta T)$. The obstacle trajectories are also discretized as $\hat{z}_i(k;s) := \hat{z}_i(k\Delta T;s)$. Although the full state trajectory $x(k)$ can be high-dimensional, homotopy class constraints are only applied to $p(k)$, which is a 2-dimensional system trajectory. Therefore, the optimal motion planning problem can then be framed as the NLP

$$\begin{aligned} \underset{(U,X)}{\text{minimize}} \quad & \|U\|^2 \\ \text{subject to} \quad & x(0) = x_{\text{start}},\ x(N) = x_{\text{target}} \\ & x(k+1) = F(x(k), u(k)) \\ & G(g(x(k)), \hat{z}_i(k;s)) \geq 0 \\ & \forall k \in \{0,\dots,N\}, i \in \{1,\dots,M\}, \end{aligned} \tag{8}$$

where $X = [x(0),\dots,x(N)]$, $U = [u(0),\dots,u(N-1)]$, and $G(g(x(k)), \hat{z}_i(k;s))$ is the control barrier function described in constraint (1). In our following experiments, the interior point optimizer is utilized to address such NLP (8). And the convergence analysis of the solver can be seen in [13].

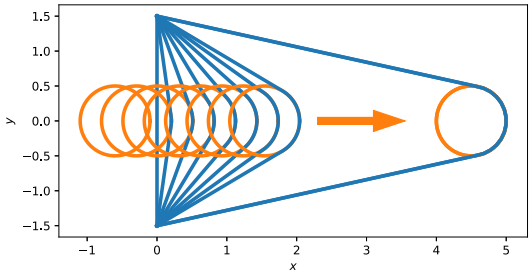

Fig. 4. Orange circles represent the obstacles and blue curves represent the synthesized shortest path in each iteration. In each iteration, the computed optimal trajectory is seen to stay on the right side of the obstacle, which fulfills the control barrier constraints.

B. Homotopy Method

As mentioned in Section III, resolving the motion planning problems with non-differentiable homotopy class constraints is equivalent to resolving the sequential differentiable motion planning problems. The auxiliary obstacle trajectory initialization can be simply achieved by choosing a large enough s_0, and the challenging task is to ensure that the system trajectory and obstacles remain untouched during the continuous deformation of the auxiliary obstacle trajectory by decreasing the push distance s, as specified in Corollary 2.

To address the challenge, we adopt the idea of the homotopy method [14] which first solves the simpler problems that are deformed from the original and complicated problem, and then gradually leverages the intermediate results to solve the ones all the way back to the original problem. In this process, we take advantage of the fact that if the local optimal trajectory is already synthesized, then obstacles are moved by a small distance and the solver uses the last result as initial values, the solver tends to provide the nearest local optimal solution. To illustrate the adapted homotopy method to our problem, we utilize a simple motion planning problem shown in Figure 4. In this example, we attempt to solve an energy-optimal motion planning problem concerning a simple system $\dot{x} = u$ and a circle obstacle that is centered at $(4.5, 0)$ with the radius of 0.5, such that the system starts from $(0, -1.5)$ to $(0, 1.5)$ and bypasses the obstacle on its right side. Instead of directly solving this hard-to-address problem, we first solve an easier problem that places the obstacle center at $(0, 0)$. Based on this intermediate result, we then solve the problem that moves the obstacle a bit right to $(0.1, 0)$. By iterating this procedure, the problem will be gradually deformed to the original one that can be easily solved based on results from the previous iteration.

The proposed approach is summarized in Algorithm 1. To choose the initial value of s, we first set it as zero and gradually increase it until no collision happens and the initial system trajectory $p(t)$ and the given trajectory $r(t)$ are in the same homotopy class towards auxiliary obstacle trajectories by checking whether the criterion (4) is satisfied. Corollary 1 guarantees the existence of such s, while it is worth noting that a small value of s will decrease the efficiency of the method. To find a suitable value of Δs, we may start from a large value of it and update obstacle trajectories and the system trajectory. If the homotopy class constraints are not satisfied with the updated trajectory, we can return to the last step and try a smaller Δs. But setting $\Delta s = \min_i R_i/5$ is found to be

Algorithm 1 Homotopy Method for Homotopy Class Constraints

Require: Obstacle trajectories $\{z_1(k), ..., z_M(k)\}$ and pre-established trajectory $r(k)$ which defines the required homotopy class.
1: Initialize inputs U^0 and state trajectory X^0 by solving (8) without considering obstacles.
2: Synthesis trajectories for obstacles $\{\hat{z}_1(k; s), ..., \hat{z}_M(k; s)\}$ according to (5) with s large enough.
3: Set iteration step $m = 0$.
4: Set $s = \max(s - \Delta s, 0)$, $m = m + 1$
5: Solve optimal motion planning problem (8) with obstacles and initial $(U, X) = (U^{m-1}, X^{m-1})$, and the solution of it is noted as (U^m, X^m).
6: Repeat step $4 - 5$ until $s = 0$.

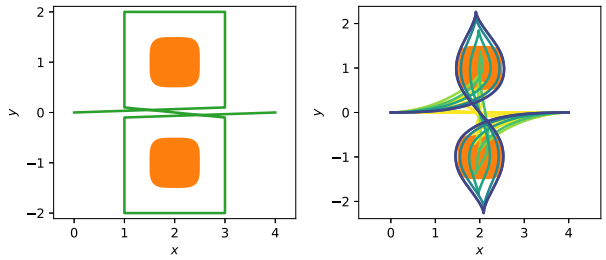

Fig. 5. The optimal trajectory is synthesized for a unicycle system with two stationary obstacles centered at $(2, -1)$ and $(2, 1)$ with $R = 0.5$ and $k = 4$. The initial and target points of the system are set to $(0, 0)$ and $(4, 0)$, respectively. The left figure shows the stationary obstacles (orange) and the given trajectory (green) in the $x - y$ plane. The right figure illustrates how the initial system trajectory (yellow) gradually deforms into the optimal trajectory (blue) that obeys the homotopy class constraints.

good in practice. To prevent obstacles from passing through the discrete trajectory and moving to another homotopy class, sample points of the system trajectory should be dense enough by choosing suitable ΔT.

V. Numerical Results

We present numerical results on two classic dynamical systems: the unicycle and the quadcopter. The results demonstrate that the proposed approach can iteratively synthesize optimal trajectories with homotopy class constraints for nonholonomic unicycle systems and highly nonlinear quadcopter systems.

A. Unicycle

We first adopt the unicycle model

$$\frac{d}{dt}\begin{pmatrix} x \\ y \\ \phi \end{pmatrix} = \begin{pmatrix} v\cos\phi \\ v\sin\phi \\ \omega \end{pmatrix},$$

as a classical nonholonomic system to illustrate optimal trajectory generation under homotopy class constraints. Here x and y indicate the position of the unicycle, and ϕ denotes the facing angle of the unicycle. Moreover, v and ω are control inputs that stand for the moving and steering velocity, respectively.

In the following demonstrations, the homotopy class constraints are applied to the position states. The facing angle ϕ is set to zero at both the start and target points. Figure 5 shows the results of the advocated approach that addresses

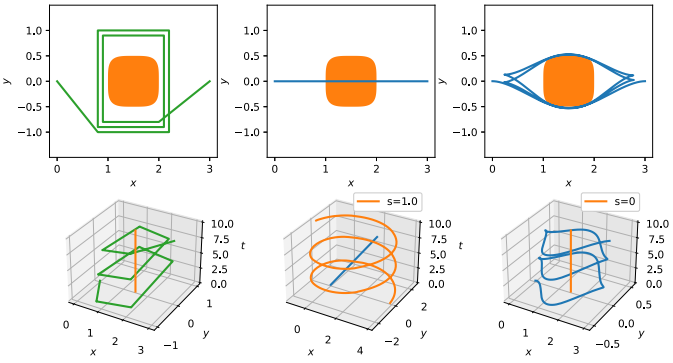

Fig. 6. The optimal trajectory is synthesized for a unicycle system with one stationary obstacle centered at $(1.5, 0)$ with $R = 0.5$ and $k = 4$. The start and target point of the system are $(0, 0)$ and $(3, 0)$, respectively. The upper row shows the given trajectory (green), the system trajectory (blue) and an obstacle (orange) in the $x - y$ plane, while the lower row presents the corresponding trajectory in the $x - y - t$ space. The middle column indicates the initial trajectories with $s = 1.0$, and the right column shows the final results.

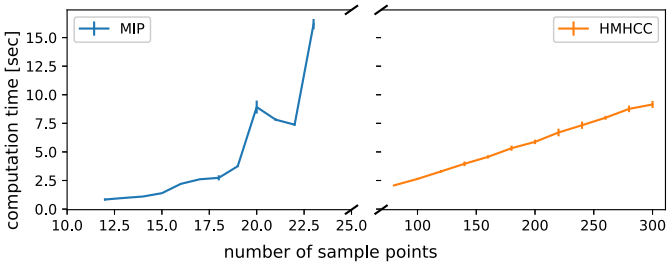

Fig. 7. Comparison of the computation time between two methods. The error distribution at each number of sample points is estimated based on 5 simulations. The computation time of MIP is not increase monotonically because the Branch-and-Bound method is leveraged to solve MIP problems.

the energy-optimal motion planning problems for a unicycle system, where the unicycle is requested to encircle two stationary obstacles before reaching the target. The total time is 10 seconds and the discrete time interval is set as $\Delta T = 0.05$ second. In addition, the push distance s is decreased from 2.5 to 0 with a step of $\Delta s = 0.1$. Another simulation with one obstacle and a different homotopy class is carried out on the same system and setups except that s is initialized as 1.0, whose results are presented in Figure 6.

We additionally compare the computational efficiency of our proposed method with the MIP-based method, which is shown in Figure 7. We attempt to leverage both methods on the same motion planning problems shown in Figure 6 but with varying sample points number, $N = T/\Delta T$, by changing ΔT. Because of the larger gap between each adjacent sample points of the trajectory, smaller N tends to result in a trajectory that violates the obstacle constraints. Due to the exponentially-like growing computation complexity of the MIP-based method, our method enjoys the fulfillment of the obstacle constraints with reasonable computation time.

B. Quadcopter

Here we consider a holonomic but highly-nonlinear quadcopter model that is described by the nonlinear dynamics with 12 states and 4 control inputs denoting the rotating speed of

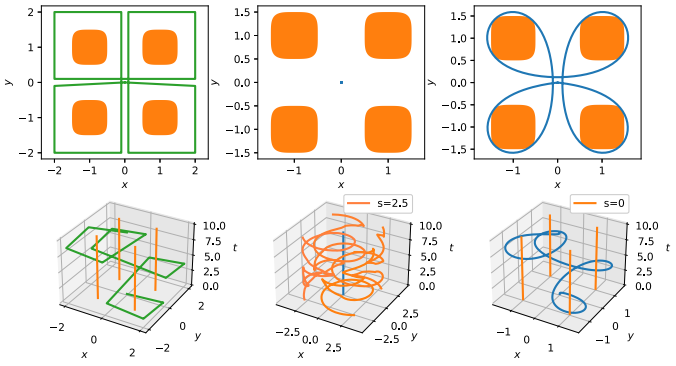

Fig. 8. The optimal trajectory is synthesized for a quadcopter system with four stationary obstacles centered at $(\pm 1, \pm 1)$ with $R = 0.5$ and $k = 4$. The start and target point of the system trajectory are set at $(0, 0)$. The layout and explanation of the figure are identical to Figure 6, except that the push distance is initialized as $s = 2.5$.

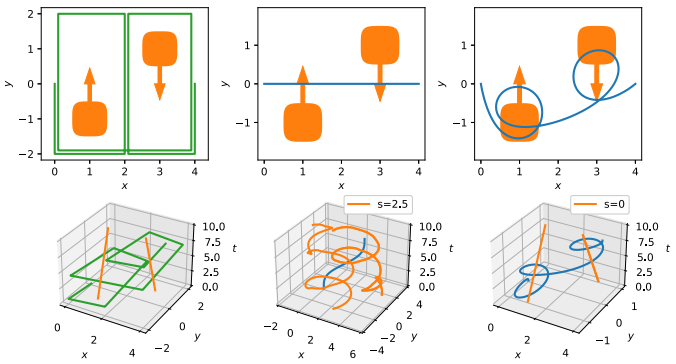

Fig. 9. The optimal trajectory is synthesized for a quadcopter system with two moving obstacles, which are originally centered at $(1, -1)$ and $(3, 1)$ with $R = 0.5$ and $k = 4$ with a constant moving speed at 0.1 m/s, and the moving direction is indicated by the orange arrow. The start and target point of the system are set at $(0, 0)$ and $(4, 0)$, respectively. The layout and explanation of the figure are identical to Figure 6, except that the push distance is initialized as $s = 2.5$.

four motors in rotation per minute and takes the form

$$\frac{d}{dt}x = f_d(x) + \sum_{i=1}^{4} f_i(x)(u_i + u_{eq})^2,$$

where $u = [u_1, u_2, u_3, u_4]^T$ are control inputs, f_d and f_i are differentiable functions. u_{eq} is the hovering motor speed, such that $(x, u) = (\mathbf{0}_{12\times 1}, \mathbf{0}_{4\times 1})$ is the equilibrium point of the dynamical system. Readers are referred to [15] for the detailed dynamics structure. According to the definition of the homotopy class in Section II-C, the constraints considered here are only applied to the $x - y$ plane, which means the altitude of the quadcopter is not concerned. As for the initial and target points, all states besides x_1 and x_2 are set to zero.

Figure 8 presents the numerical results for a quadcopter flight in a cluttered environment with four stationary obstacles. The total time needed is set as $T = 10s$ and the time interval as $\Delta T = 0.05s$. In addition, the push distance is gradually decreased from $s = 2.5$ to $s = 0$ with $\Delta s = 0.05$. In Figure 9, the algorithm is applied to the same system with the same experimental setups, whereas two moving obstacles are considered instead. The results suggest that the proposed method is further capable of addressing the homotopy-constrained optimal motion planning problems with moving obstacles.

VI. Conclusion

In this letter, we introduced a novel optimal motion planning technique with 2-dimensional homotopy class constraints. It first initializes the dynamical system trajectory such that it belongs to the desired homotopy class regarding the auxiliary obstacle trajectories rather than the original obstacles. By gradually deforming the auxiliary ones to their original counterparts, the dynamical system trajectory fulfilling the homotopy property and the corresponding inputs are eventually synthesized. We have demonstrated the practicability of the proposed method on nonholonomic systems with both static and moving obstacles. However, the current method is limited to the planer homotopy class constraints, which remains to be addressed in the future.

References

[1] L. E. Kavraki, P. Svestka, J.-C. Latombe, and M. H. Overmars, "Probabilistic roadmaps for path planning in high-dimensional configuration spaces," *IEEE Trans. Robot. Autom.*, vol. 12, no. 4, pp. 566–580, Aug. 1996.

[2] J. J. Kuffner and S. M. LaValle, "RRT-connect: An efficient approach to single-query path planning," in *Proc. ICRA Millennium Conf. IEEE Int. Conf. Robot. Autom. Symposia*, vol. 2, 2000, pp. 995–1001.

[3] M. Vu and S. Zeng, "Iterative optimal control syntheses for nonlinear systems in constrained environments," in *Proc. Amer. Control Conf. (ACC)*, 2020, pp. 1731–1736.

[4] K. Bergman and D. Axehill, "Combining homotopy methods and numerical optimal control to solve motion planning problems," in *Proc. IEEE Intell. Veh. Symp. (IV)*, 2018, pp. 347–354.

[5] J. Park, S. Karumanchi, and K. Iagnemma, "Homotopy-based divide-and-conquer strategy for optimal trajectory planning via mixed-integer programming," *IEEE Trans. Robot.*, vol. 31, no. 5, pp. 1101–1115, Oct. 2015.

[6] D. Grigoriev and A. Slissenko, "Polytime algorithm for the shortest path in a homotopy class amidst semi-algebraic obstacles in the plane," in *Proc. Int. Symp. Symb. Algebr. Comput.*, 1998, pp. 17–24.

[7] S. Bhattacharya, V. Kumar, and M. Likhachev, "Search-based path planning with homotopy class constraints," in *Proc. AAAI Conf. Artif. Intell.*, vol. 24, 2010, pp. 1230–1237.

[8] R. Kala, "Homotopic roadmap generation for robot motion planning," *J. Intell. Robot. Syst.*, vol. 82, nos. 3–4, pp. 555–575, 2016.

[9] S. Kim, K. Sreenath, S. Bhattacharya, and V. Kumar, "Optimal trajectory generation under homology class constraints," in *Proc. IEEE 51st IEEE Conf. Decis. Control (CDC)*, 2012, pp. 3157–3164.

[10] W. He, Y. Huang, and S. Zeng, "Motion planning with Homotopy class constraints via the auxiliary energy reduction technique," in *Proc. Amer. Control Conf. (ACC)*, Atlanta, GA, USA, Jun. 2022, pp. 4933–4938.

[11] M. J. Ablowitz, A. S. Fokas, and A. S. Fokas, *Complex Variables: Introduction and Applications*. Cambridge, U.K.: Cambridge Univ. Press, 2003.

[12] J. A. E. Andersson, J. Gillis, G. Horn, J. B. Rawlings, and M. Diehl, "CasADi: A software framework for nonlinear optimization and optimal control," *Math. Program. Comput.*, vol. 11, no. 1, pp. 1–36, 2019.

[13] I. Griva, D. F. Shanno, and R. J. Vanderbei. "Convergence analysis of a primal-dual interior-point method for nonlinear programming." Optimization Online. 2004. [Online]. Available: http://www.optimizationonline.org/DB HTML/2004/07/913.html

[14] R. Horst and P. M. Pardalos, *Handbook of Global Optimization*. London, U.K.: Kluwer Acad. Publ., 1995.

[15] F. Sabatino, "Quadrotor control: Modeling, nonlinear control design, and simulation," M.S. thesis, Dept. Electr. Eng., KTH Royal Inst. Technol., Stockholm, Sweden, 2015.